Electronic Supporting Information for

Microfluidic Electrosynthesis of Thiuram Disulfides

Siyuan Zheng, Kai Wang* and Guangsheng Luo

The State Key Lab of Chemical Engineering, Department of Chemical Engineering, Tsinghua University, Beijing 100084, China

*Corresponding author email: kaiwang@tsinghua.edu.cn

Experimental platforms

1. Batch electrolyser for cyclic voltammetry and potentiostatic electrolysis experiments

The measurement of cyclic voltammetry and potentiostatic electrolysis experiments in batch reactor were carried out in a 3-electrode reactor (250 mL) with a platinum anode, a platinum cathode, and a saturated calomel reference electrode as shown in Figure S1. In this reactor, the area of anode was 1 cm^2 and the area of cathode was 2.25 cm^2. The organic and aqueous solutions were mixed by a magnetic stirrer (85-2, TIANLI). The potential and the scan rate of the electrolysis reaction were controlled by an electrochemical workstation (PARSTAT 3000A-DX, AMETEK Inc.).

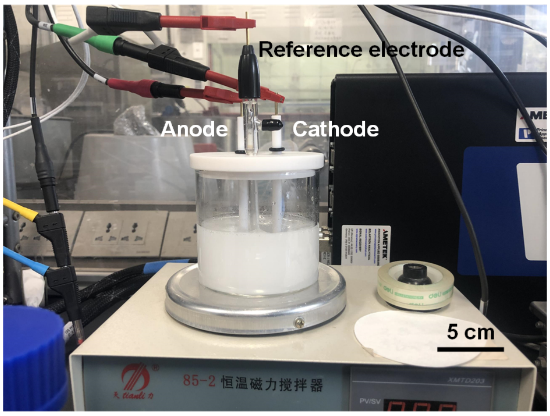

Figure S1. Photo of the batch electrolyser and the electrodes in experiment.

2. Microfluidic electrosynthesis platform for the preparation of thiuram disulfides

As the core component of electrosynthesis platform, the microfluidic electrolysis reactor has a multilayer structure as shown in Figure S2(a). The height of microchannel was controlled to 0.3 mm by the thickness of the fluorinated ethylene propylene (FEP) channel plate in the experiment. 61, 97, and 245 mm long microchannels with 2 mm width were fabricated on those plates with a CO_2 laser cutter (JK-100W, HUITIAN Laser). Two 3.5 cm × 3.5 cm platinum electrodes (Pt purity >99.99%) with welding wires were placed on both sides of the channels, and they were sealed with the channel plate with 0.5 mm Teflon plates. Out of the sealing plates, two polyvinylidene fluoride (PVDF) modules were used as the connection components, and two modules made from polyetheretherketone (PEEK) or aluminum were assembled as the shells of the reactor for screw sealing. Both the PVDF modules and the PEEK/Al shells were self-designed, and fabricated by HUAJIAOZHENBANG Company in Beijing. Figure S2(b) shows the assembled microfluidic reactor connected with the electrochemical workstation (PARSTAT 3000A-DX, AMETEK Inc.). Both the connection tubes and the wires were sealed by commercial fittings from Idex Health & Science. To feed the microfluidic electrolysis reactor, the mixture of toluene and sodium dithiocarbamate solution was created by the biphasic mixer assembled from a PEEK Tee-connector (1 mm inner diameter, Idex Health & Science), as shown in Figure S2(c). A stainless-steel capillary with 0.6 mm outer diameter and 0.4 mm inner diameter was embedded in the connector, and formed the inner tube of the mixer, which was used to feed the sodium dithiocarbamate solution. The annular space between the inner tube and the flow path in the Tee-connector was used to feed toluene. Toluene was injected from the branched hole of the connector and it cut the aqueous phase at the tip of the stainless-steel capillary forming liquid-liquid Taylor flow [1,2], which were regular droplet flows in the downstream tube with 1.0 mm inner diameter and 1.6 mm outer diameter (perfluoroalkoxy alkanes, PFA, Idex Health & Science). A complete picture of the microfluidic electrolysis platform is shown in Figure 2(d). All the solutions were driven by continuous syringe pumps (MSP1-E1, Longer). Experimental temperature at 25ºC (±1ºC) was controlled by the air conditioning system.

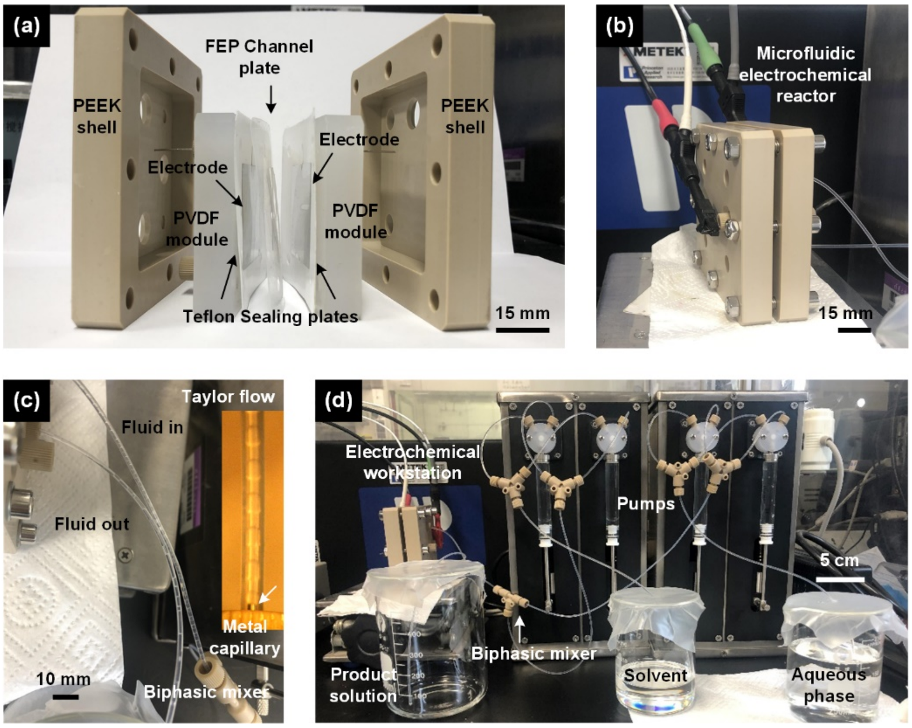

Figure S2. Photos of the microfluidic electrolysis platform. (a) The core components of the microfluidic electrolysis reactor. (b) The assembled reactor. (c) The connection tubes of the reactor. Right figure shows the metal capillary in the biphasic mixer and the uniform droplets in the connection tube. (d) The whole platform of the microfluidic electrosynthesis reaction.

To increase the productivity of the microfluidic electrolysis reactor, we applied paralleled microfluidic reactors in the experiment as shown in Figure S3. Each microfluidic electrolysis reactor in this picture had the same inner structure with 0.3 mm reaction channel height, 245 mm channel length, and 2 mm channel width. Two 3.5 cm × 3.5 cm platinum electrodes (Pt purity >99.99%) were placed on both sides of the channels. The only difference of the two reactors was the shell material (PEEK and Al), which do not influence the reaction. The two reactors were fed individually by continuous syringe pumps and independently controlled by the two channels of the electrochemical workstation (PARSTAT 3000A-DX, AMETEK Inc.)

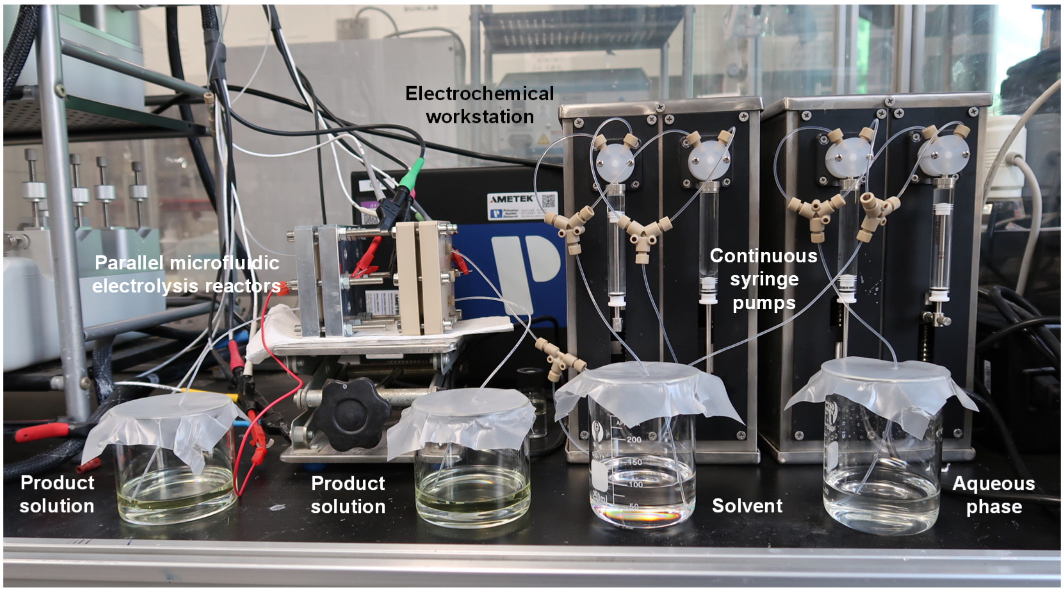

Figure S3. Photo of the paralleled microfluidic electrolysis reactors in experiment.

3. Packed bed reactor platform for the preparation of sodium dithiocarbamates

To turn the aqueous solution after electrolysis into the source of the electrolysis reaction, packed bed reactors were developed to prepare sodium dithiocarbamate solutions from the reaction of sodium hydroxide, secondary amine, and carbon disulfide. Figure S4 shows the platform. The packed bed reactor was assembled from an empty HPLC column (316L stainless-steel, BAIJIALIDA Co., Ltd.) with 4.6 mm inner dimeter and 100 mm length. The column was fully filled by 0.9 mm stainless-steel (304L) beads. The void ratio of the reactor bed was 44.6 %. To synthesize sodium dibutyldithiocarbamate ($NaBu_2DTC$), a cross-connector (316L stainless-steel, VICI – Valco) with 0.5 mm inner diameter was used to mix the recycled NaOH solution, dibutylamine, and CS_2, which were fed by syringe pumps (Fusion 6000 and 4000, Chemyx) as shown in the figure. In the cases of sodium diethyldithiocarbamate ($NaEt_2DTC$) and sodium dimethyldithiocarbamate ($NaMe_2DTC$) syntheses, diethylamine and dimethylamine were pre-dissolved into the recycled solutions; therefore, a Tee-connector (316L stainless-steel, VICI – Valco, not shown in the photo) was used instead of the cross connector, and only two syringes were employed to fed the reactants. Experimental temperature at 25ºC (±1ºC) was controlled by the air conditioning system.

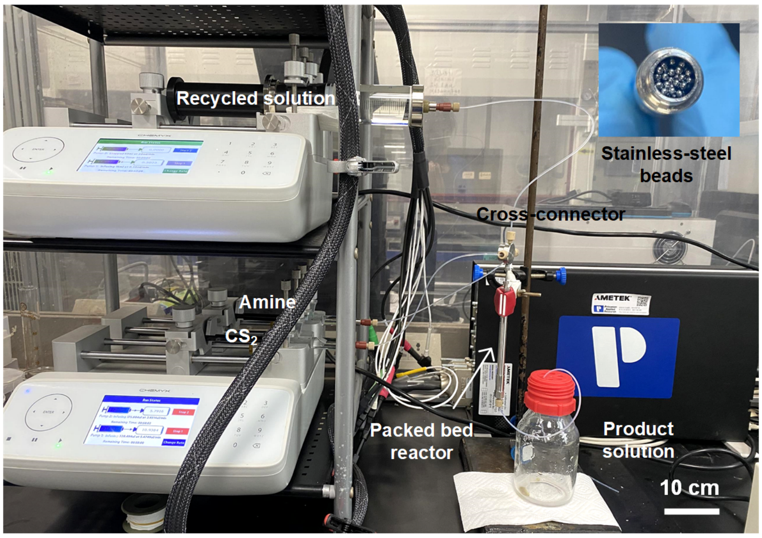

Figure S4. Photo of the packed bed reactor to generate sodium dithiocarbamate solutions from the aqueous solutions after electrolysis.

Experimental results of the electrosynthesis processes

1. Contact angle measurements of liquid-liquid systems on platinum electrode

As a multiphase reaction system, the electrosynthesis reaction should be influenced by the fluid wetting property on electrodes. Contact angle measurements were thus carried out to understand the wetting property of toluene on platinum. The experiments were implemented in a modified sessile droplet contact angle measurement instrument (OCAH200, Data Physics Instruments GmbH), and some typical results are shown by Figure S5. Figure S5(a) shows that platinum electrode was hydrophilic in the system containing $NaEt_2DTC$ solution and toluene. To get closer to the electrolysis reaction, a reversed sessile droplet experiment was applied as shown in Figure S5(b). 2.0 V cell potential was added on the electrodes by a DC power supply (UTP3705, UNI-T). The results show that the electrode was still hydrophilic. The contact angle of toluene was at about 100º in a 0.15 $mol{\cdot}L^{-1}$ $NaEt_2DTC$ solution. This hydrophilic property of platinum was benefit for the exposure of electrode surface to the reactant solution.

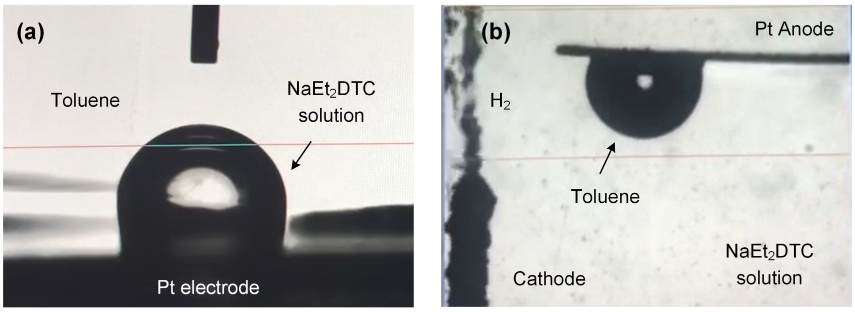

Figure S5. Photos of contact angle measurement experiments. (a) A 0.15 $mol{\cdot}L^{-1}$ $NaEt_2DTC$ solution sessile droplet on Pt electrode in toluene. (b) A reversed sessile droplet of toluene in 0.15 $mol{\cdot}L^{-1}$ $NaEt_2DTC$ solution on Pt electrode. 2.0 V voltage was applied between electrodes to simulate the reacting condition.

2. Electrode surface states after electrolysis reaction

The sediment of thiuram disulfides on the electrodes was one of the limiting factors of the electrosynthesis method; therefore, solution assisted electrolysis was developed in this study. To show the effect of solvent dissolution during the electrolysis reaction, the electrode surface was carefully observed during the experiments. Figure S6(a) is a photo of the anode after the batch electrolysis experiment with toluene as the solvent. The electrode was directly pulled up from the batch electrolyser and we can see a thin tetraethylthiuram disulfide (TETD) layer was stick on the electrode. In contrast to the batch electrolyser, where the contact of solvent and electrode was random, the liquid-liquid Taylor flow in microchannels cleaned the electrode timely, which made the electrolysis more reliable. Figure S6(b) is a picture of the anode in the microfluidic electrolysis experiment with toluene as the solvent. The reactor was directly opened after electrolysis; therefore, the evaporation of residual toluene left some traces on some part of the channel positions. If the reactor was opened after several minutes flushing by toluene, the electrode would look the same as the situation before experiment, as shown by Figure S6(c).

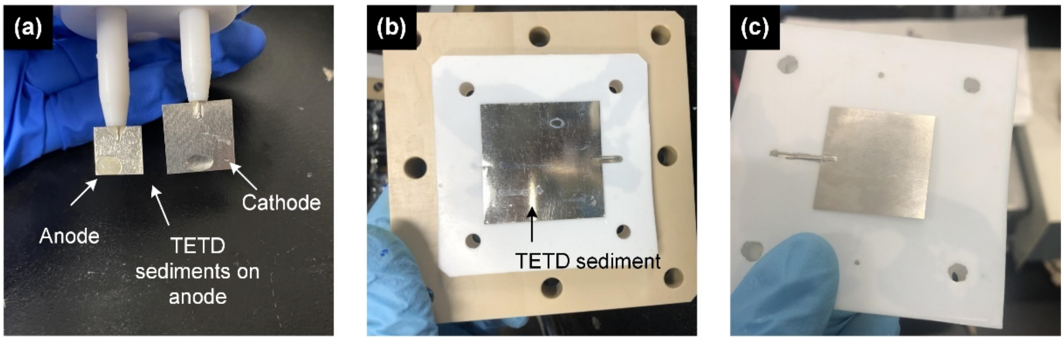

Figure S6. Photos of anodes after electrolysis. (a) The anode with a little bit TETD deposition. 100 mL 0.15 mol·L^{-1} NaEt$_2$DTC solution and 100 mL toluene were used in the batch electrolysis experiment with 2.0 V work voltage versus the reference electrode. (b) The anode with a little bit TETD traces in the microfluidic reactor without solvent flushing. Experiment was at 0.25 mL·min^{-1} NaEt$_2$DTC aqueous solution and 0.25 mL·min^{-1} toluene. NaEt$_2$DTC concentration was 0.15 mol·L^{-1} solution. 2.0 V cell potential was applied on the 0.15 mL reaction channel at 25ºC. (c) The anode without any sediment in the microfluidic reactor after 2 min flushing by toluene. Experiment conditions were the same as those of Figure S6(b).

3. Linear sweep voltammetry of sodium hydroxide solution

Linear sweep voltammetry of sodium hydroxide solution was carried out in the microfluidic reactor to understand the competitive water electrolysis reaction. As shown by Figure 7, the electrolysis reaction started at a little bit higher than 2.0 V, but the reaction rate at 2.0 V was very low. The response current became oscillating at the cell potential higher than 2.5 V, which means the appearance of a large amount of gas phase in the microchannel.

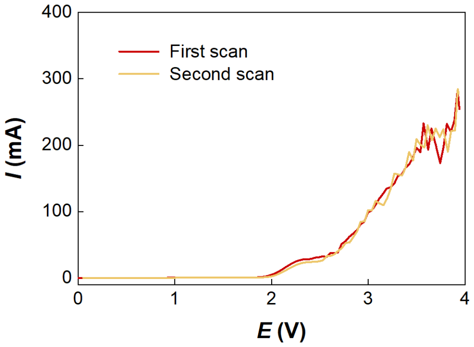

Figure S7. Positive scan of a typical sodium hydroxide aqueous solution. Experiment was at 0.05 mol·L^{-1} NaOH concentration, 0.25 mL·min^{-1} flow rate, 0.15 mL microchannel volume and 0.01 V·s^{-1} scan rate.

4. Linear sweep voltammetries of sodium dithiocarbamate solutions

Electrosyntheses of tetramethylthiuram disulfide (TMTD) and tetrabutylthiuram disulfide (TBuTD) were directly characterized in the microfluidic reactor under flow conditions. Since the solutions were continuously fed into the reaction channels, the negative scan was useless due to rushing out the reaction products. Besides, Figure 1(b) in the main text has shown the generation of thiuram disulfide is irreversible. The positive scans in Figure S8 show the current peaks of $NaMe_2DTC$ and $NaBu_2DTC$ electrolysis are at about 2.0 V, which are the same as the electrolysis of $NaEt_2DTC$. Oscillating currents should be due to the segmented flow pattern and H_2 bubbles generation in the microfluidic reactor.

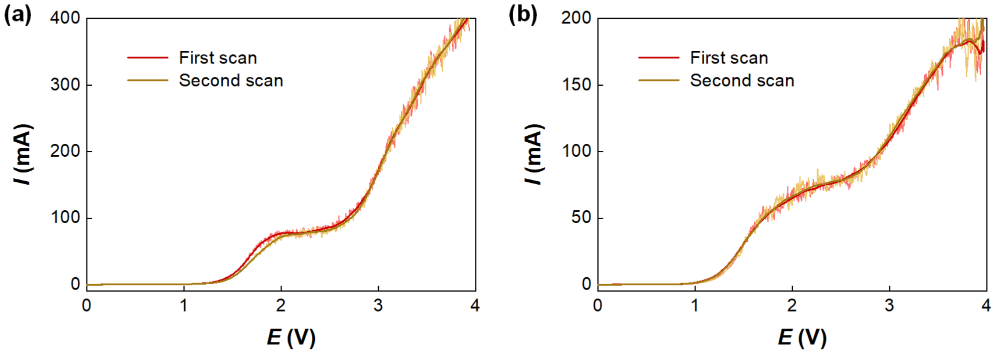

Figure S8. Positive scans of sodium dithiocarbamates in the microfluidic electrolysis reactor. (a) Experiment was at 0.15 $mol \cdot L^{-1}$ $NaMe_2DTC$ concentration, 1.0 $mL \cdot min^{-1}$ total flow rate, 1:1 flow rate ratio of liquid phases, 0.15 mL microchannel volume and 0.01 $V \cdot s^{-1}$ scan rate. (b) Experiment was at 0.15 $mol \cdot L^{-1}$ $NaBu_2DTC$ concentration, 1.0 $mL \cdot min^{-1}$ total flow rate, 1:1 flow rate ratio of liquid phases, 0.15 mL microchannel volume and 0.01 $V \cdot s^{-1}$ scan rate.

5. Microfluidic electrolysis of $NaEt_2DTC$ under galvanostatic conditions

Besides potentiostatic electrolysis experiments, the galvanostatic electrolysis experiments, which were more robust in control the reaction rate, were investigated. 10-40 mA reaction currents were applied by the electrochemical workstation. Entries 3 and 5 in Table S1 show that the galvanostatic electrolysis reactions had good reproducibility. However, the Faraday efficiencies are relatively lower than those using potentiostatic method (>96%), and the best TETD yield gained under 40 mA, when the response cell potential had been higher than 2.0 V, was lower than the best gained at 2.0 V (69%). A faraday efficiency lower than 100% means the appearance of water electrolysis. Thus, we preferred to use the potentiostatic method in this study, which aimed to develop a green method for thiuram disulfides.

Table. S1 Typical results for the electrosynthesis of TETD under galvanostatic conditions. (25ºC)

Entry	Total flow rate of liquids ($mL \cdot min^{-1}$)	Reaction channel volume (mL)	Electrolysis current (mA)	Concentration of $NaEt_2DTC$ ($mol \cdot L^{-1}$)	TETD yield (%)	Faraday efficiency (%)
1	0.5	0.15	10	0.15	16%	94%
2	0.5	0.15	20	0.15	32%	96%
3	0.5	0.15	30	0.15	46%	93%
4	0.5	0.15	40	0.15	58%	88%
5	0.5	0.15	30	0.15	47%	94%

6. Synthesis of sodium dithiocarbamates with the packed bed reactor

Similar as the continuous synthesis of $NaEt_2DTC$ solution in the packed bed reactor shown by Table 4 in the main text, typical results for $NaMe_2DTC$ and $NaBu_2DTC$ synthesis reactions are shown in Tables S2 and S3. To prepare $NaMe_2DTC$, dimethylamine was premixed into the recycled aqueous solution; thus, a Tee-connector (0.5 mm inner diameter, VICI) was employed to mix the aqueous solution and carbon disulfide, as shown by Figure 7(a). For $NaBu_2DTC$, a cross-connector (0.5 mm inner diameter, VICI) was used to mix the recycled aqueous solution, dibutylamine, and carbon disulfide instead of the Tee-connector, as shown by Figure 7(b) and Figure S4. All the experiments used a constant molar ratio of reactants at $NaOH/amine/CS_2$ = 1:1:1.5. Excessive CS_2 was separated by gravity after reaction. For all reaction systems, the packed bed reactors provided proper environments, where the NaOH conversions were close to 100% in 2.9 min residence time.

Table. S2 Results for the packed bed reaction for the synthesis of $NaMe_2DTC$ aqueous solution. (25ºC)

Entry	$NaMe_2DTC$ concentration (mol·L^{-1})	NaOH concentration (mol·L^{-1})	Dimethylamine concentration (mol·L^{-1})	Recycled liquid flow rate (mL·min^{-1})	CS_2 flow rate (μL·min^{-1})	NaOH conversion (%)	Product pH
1	0.066	0.047	0.047	0.25	1.07	99.13%	10.29
2	0.078	0.035	0.035	0.25	0.79	99.58%	9.84
3	0.072	0.041	0.041	0.25	0.92	99.45%	9.91
4	0.118	0.044	0.044	0.25	0.99	99.29%	10.05
5	0.121	0.041	0.041	0.25	0.91	99.74%	9.64

Table. S3 Results for the packed bed reaction for the synthesis of $NaBu_2DTC$ aqueous solution. (25ºC)

Entry	$NaBu_2DTC$ concentration (mol·L^{-1})	NaOH concentration (mol·L^{-1})	Recycled liquid flow rate (mL·min^{-1})	Dibutylamine flow rate (μL·min^{-1})	CS_2 flow rate (μL·min^{-1})	NaOH conversion (%)	Product pH
1	0.018	0.129	0.25	5.47	2.93	99.97%	9.18
2	0.028	0.119	0.25	5.04	2.70	99.97%	9.24
3	0.037	0.110	0.25	4.67	2.50	99.95%	9.41
4	0.053	0.094	0.25	3.98	2.13	99.95%	9.33
5	0.081	0.066	0.25	2.80	1.50	99.93%	9.41

HPLC and H^1-NMR spectra of electrolysis and condensation reaction products

1. Typical HPLC spectra for solutions in electrolysis experiments

Figure S9 shows typical HPLC spectra of $NaEt_2DTC$ electrolysis experiments using the batch reactor. For the microfluidic electrolysis experiments, the spectra are almost the same; thus, only the result of a typical batch reaction is shown here. The electrolysis reaction was carried out with a system containing 100 mL 0.15 mol·L^{-1} $NaEt_2DTC$ solution and 100 mL toluene. The electrolysis potential was 2.0 V. After 100 min electrolysis, product solutions shown in Figure S9 were obtained. Figure S9(a) shows that the original $NaEt_2DTC$ solution before electrolysis, which contained a little bit of TETD that was probably from the oxidation of $NaEt_2DTC$ by air in storage. A little bit of TETD also existed in the aqueous product solution as shown in Figure S9(b), which should be because of the distribution of TETD between the organic phase and the aqueous phase. The $NaEt_2DTC$ peak in Figure S9(b) reduces obviously in contrast to that in Figure S9(a). Figure S9(c) shows that the organic phase contains toluene and TETD. Although the peak area of TETD looks the same as those in the aqueous phase, we should notice that the sample of organic phase had been diluted 51 times, which was much more than the twice dilution of the aqueous phase.

The same as the electrosynthesis of TETD, the electrosyntheses of TMTD and TBuTD in the microfluidic reactor also worked well in selectivity. Typical results of $NaMe_2DTC$ electrolysis are shown in Figure S10. Experiment was carried out at a total liquid flow rate of 0.5 mL·min^{-1}, 1:1 flow rate ratio of liquid phases, 0.11 mol·L^{-1} $NaMe_2DTC$, 2.0 V cell potential, 0.06 mL reactor channel volume, and 25 ºC. Besides of $NaMe_2DTC$ and TMTD, a little bit impurity can be observed in the spectrum of original $NaMe_2DTC$ solution, and no additional impurity peak is found in the aqueous phase product. TMTD comes out earlier than toluene in the spectrum for its higher polarity. Due to weaker polarity of TBuTD, the mobile phase of HPLC was changed to 100% acetonitrile and 220 nm detection wavelength was used to fit for the best absorbance of TBuTD. However, because of the mobile phase variation, the peak of $NaBu_2DTC$ changed to an irregular shape as shown by Figure S11(a). However, this shape does not take place to the other peaks. Experiment for Figure S11 was carried out at a total liquid flow rate of 0.5 mL·min^{-1}, 1:1 flow rate ratio of liquid phases, 0.15 mol·L^{-1} $NaBu_2DTC$, 2.0 V cell potential, 0.15 mL reactor channel volume, and 25 ºC. Few peaks of impurities can be found in the product solutions.

2. Typical HPLC spectra for sodium dithiocarbamate solutions from packed bed reaction

To further demonstrate the cyclic reaction craft, the aqueous phases after electrolysis were converted to the source solutions for electrolysis via the packed bed reactors shown in Figures 7 and S4. Figure S12 shows the typical HPLC spectra of $NaEt_2DTC$, $NaMe_2DTC$, and $NaBu_2DTC$ solutions. Compared to Figures S9(a), S10(a), and S11(a), the spectra in Figure S12 are almost the same as the corresponding ones prepared from purchased chemicals.

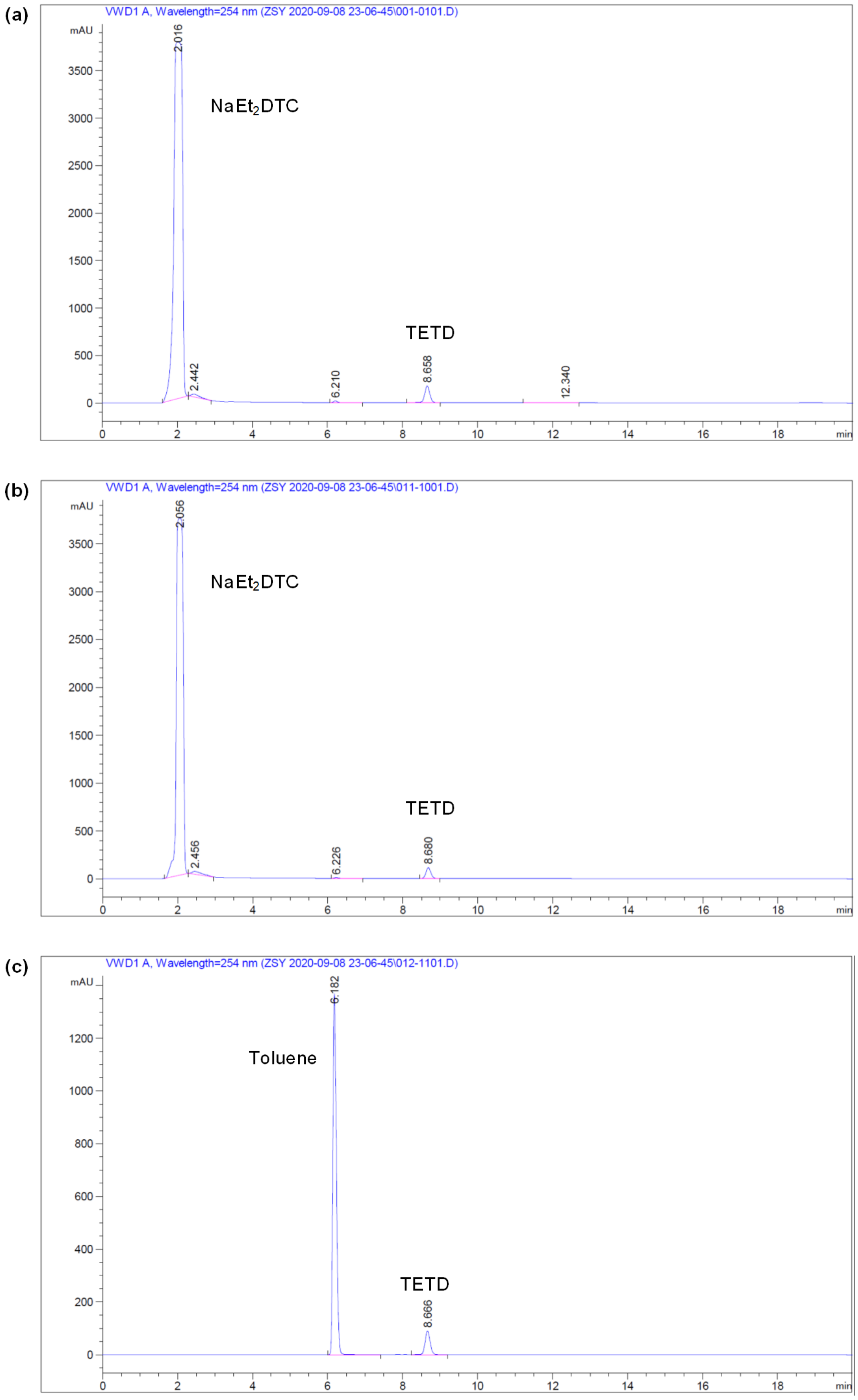

Figure S9. HPLC spectra of the original and product solutions in the $NaEt_2DTC$ electrolysis experiment. (a) HPLC spectrum of the $NaEt_2DTC$ original solution with a concentration of 0.15 mol·L^{-1}. 5 μL sample from twice dilution of the original solution. (b) HPLC spectrum of the $NaEt_2DTC$ solution after electrolysis. 5 μL sample from twice dilution of the product solution. (c) HPLC spectrum of the organic solution after electrolysis. 5 μL sample from 51 times dilution of the product solution. Experiment was carried out by using 100 mL 0.15 mol·L^{-1} $NaEt_2DTC$ solution and 100 mL toluene in the batch reactor with 2.0 V electrolysis potential and 100 min electrolysis time.

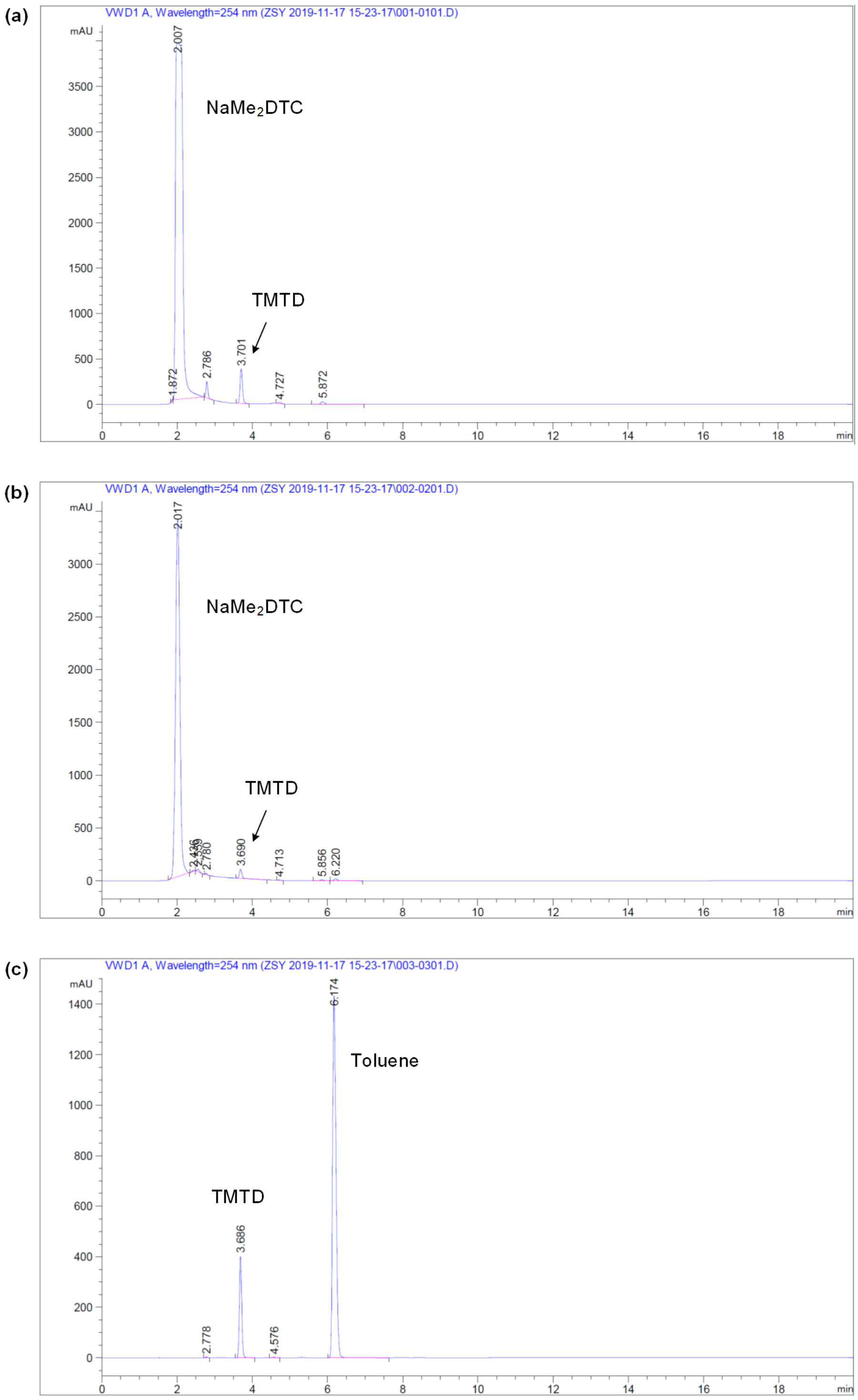

Figure S10. HPLC spectra of the original and product solutions in the $NaMe_2DTC$ electrolysis experiment. (a) HPLC spectrum of the $NaMe_2DTC$ original solution with a concentration of 0.11 $mol\cdot L^{-1}$. 5 μL sample from twice dilution of the original solution. (b) HPLC spectrum of the $NaMe_2DTC$ solution from microfluidic electrolysis reaction. 5 μL sample from twice dilution of the product solution. (c) HPLC spectrum of the organic solution from microfluidic electrolysis reaction. 5 μL sample from 51 times dilution of the product solution. Experiment was at a total liquid flow rate of 0.5 $mL\cdot min^{-1}$, 1:1 flow rate ratio of liquid phases, 2.0 V cell potential, 0.06 mL reactor channel volume, and 25ºC.

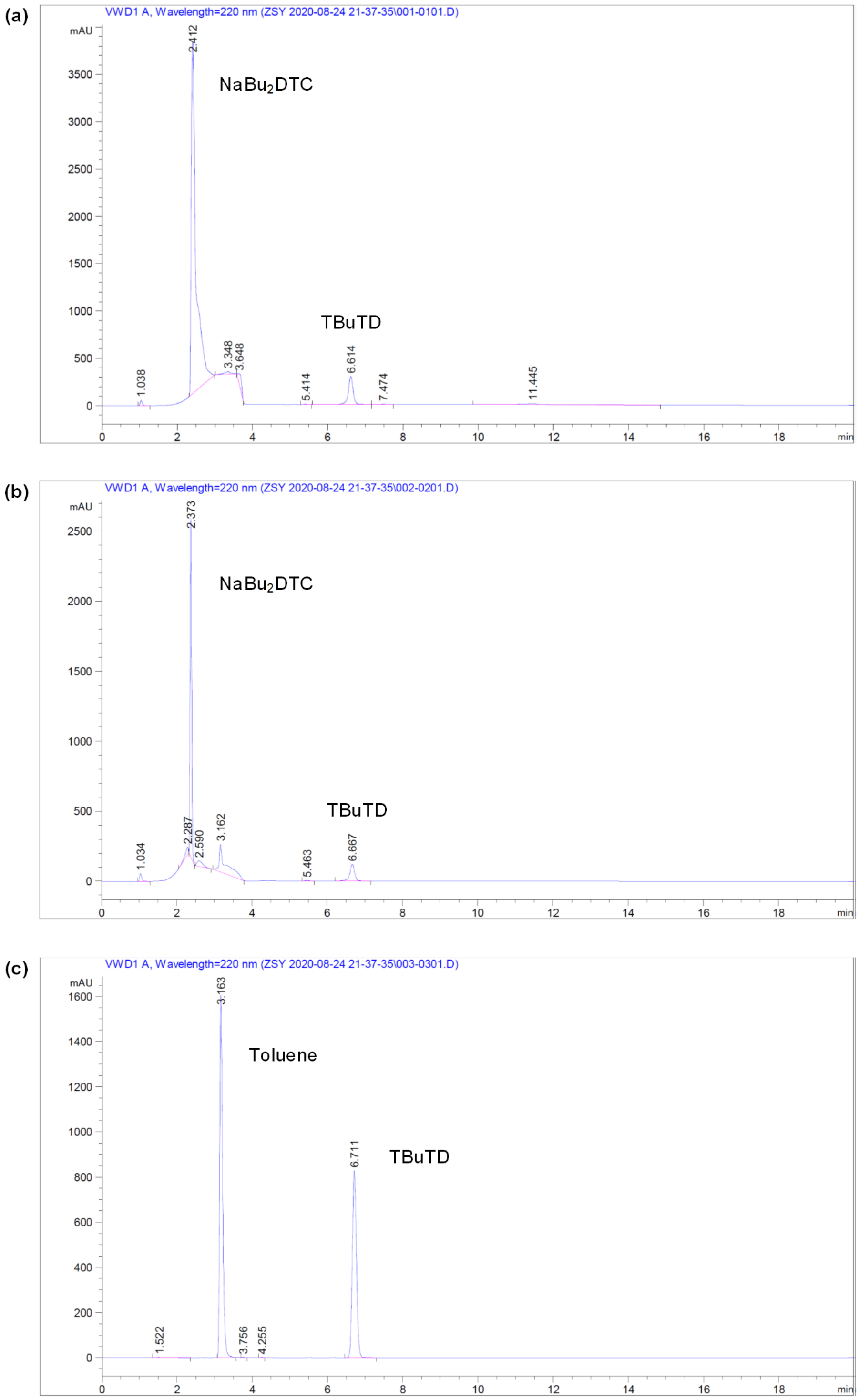

Figure S11. HPLC spectra of the original and product solutions in the $NaBu_2DTC$ electrolysis experiment. (a) HPLC spectrum of the $NaBu_2DTC$ original solution with a concentration of 0.15 mol·L^{-1}. 5 μL sample from twice dilution of the original solution. (b) HPLC spectrum of the $NaBu_2DTC$ solution from microfluidic electrolysis reaction. 5 μL sample from twice dilution of the product solution. (c) HPLC spectrum of the organic solution from microfluidic electrolysis reaction. 5 μL sample from 51 times dilution of the product solution. Experiment was at a total liquid flow rate of 0.5 mL·min^{-1}, 1:1 flow rate ratio of liquid phases, 2.0 V cell potential, 0.15 mL reactor channel volume, and 25ºC.

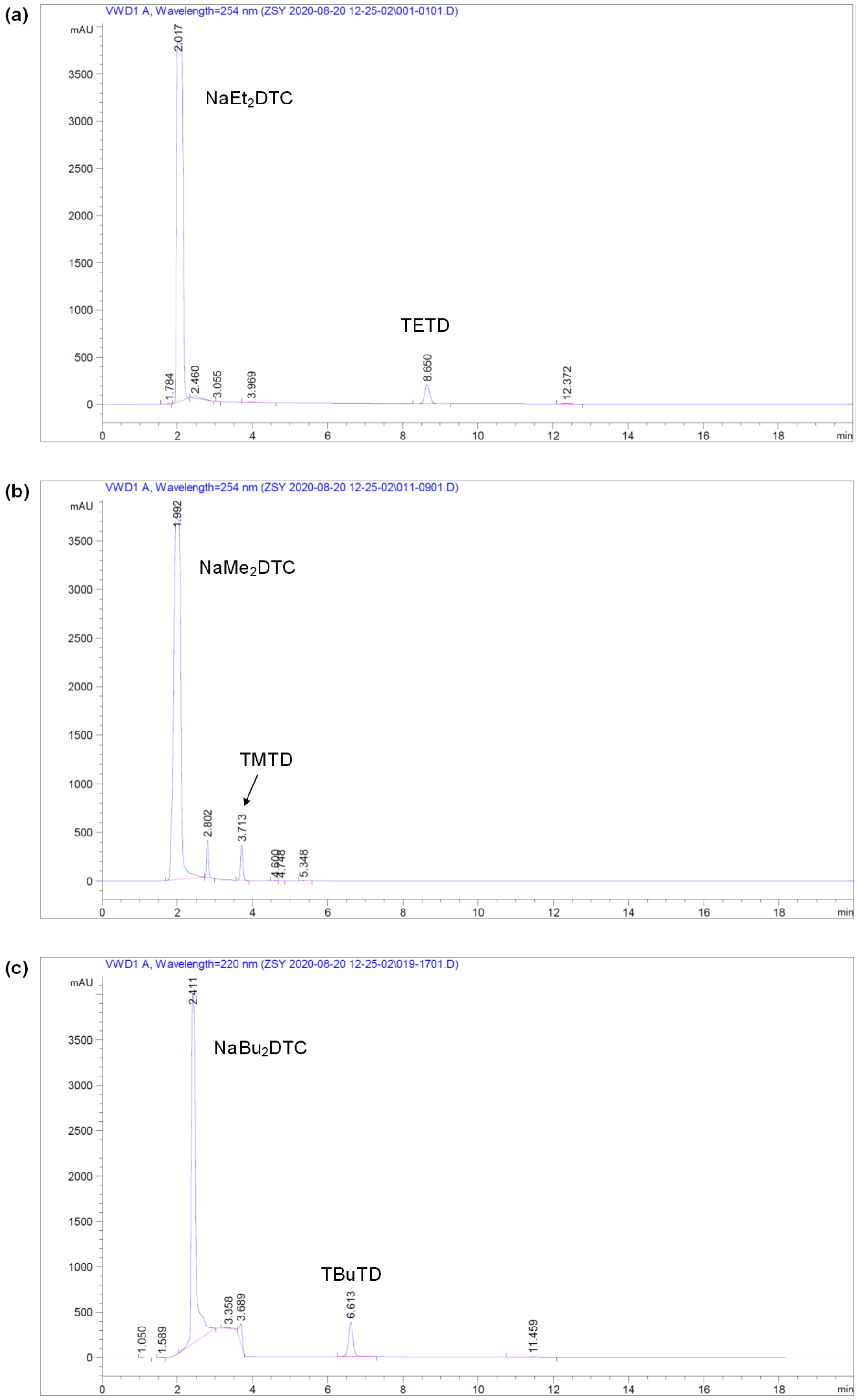

Figure S12. HPLC spectra of the product solutions from the packed bed reaction experiments. (a) HPLC spectrum of the NaEt$_2$DTC solution from the experiment with 2.47 μL·min^{-1} CS$_2$ and 0.25 mL·min^{-1} recycled solution containing 0.04 mol·L^{-1} NaEt$_2$DTC, 0.11 mol·L^{-1} NaOH, and 0.11 mol·L^{-1} diethylamine. 5 μL sample from twice dilution of product solution. (b) HPLC spectrum of the NaMe$_2$DTC solution from the experiment with 1.07 μL·min^{-1} CS$_2$ and 0.25 mL·min^{-1} recycled solution containing 0.066 mol·L^{-1} NaMe$_2$DTC, 0.047 mol·L^{-1} NaOH, and 0.047 mol·L^{-1} dimethylamine. 5 μL sample from twice dilution of product solution. (b) HPLC spectrum of the NaBu$_2$DTC solution from the experiment with 2.13 μL·min^{-1} CS$_2$, 3.98 μL·min^{-1} dibutylamine, and 0.25 mL·min^{-1} recycled solution containing 0.053 mol·L^{-1} NaBu$_2$DTC and 0.094 mol·L^{-1} NaOH. 5 μL sample from twice dilution of product solution.

3. H^1-NMR spectra of thiuram disulfides

To further confirm the structure and purity of the products we prepared, we isolated the TMTD, TETD and TBuTD in the organic phase by vacuum distillation with a Schlenk system and did H^1-NMR analysis of those samples by Bruker AVANCEIII 400 HD with comparison towards the commercial products. Figure S13 shows the results. It can be seen from the figure that our products have the same peaks as the commercial ones without any byproduct peaks.

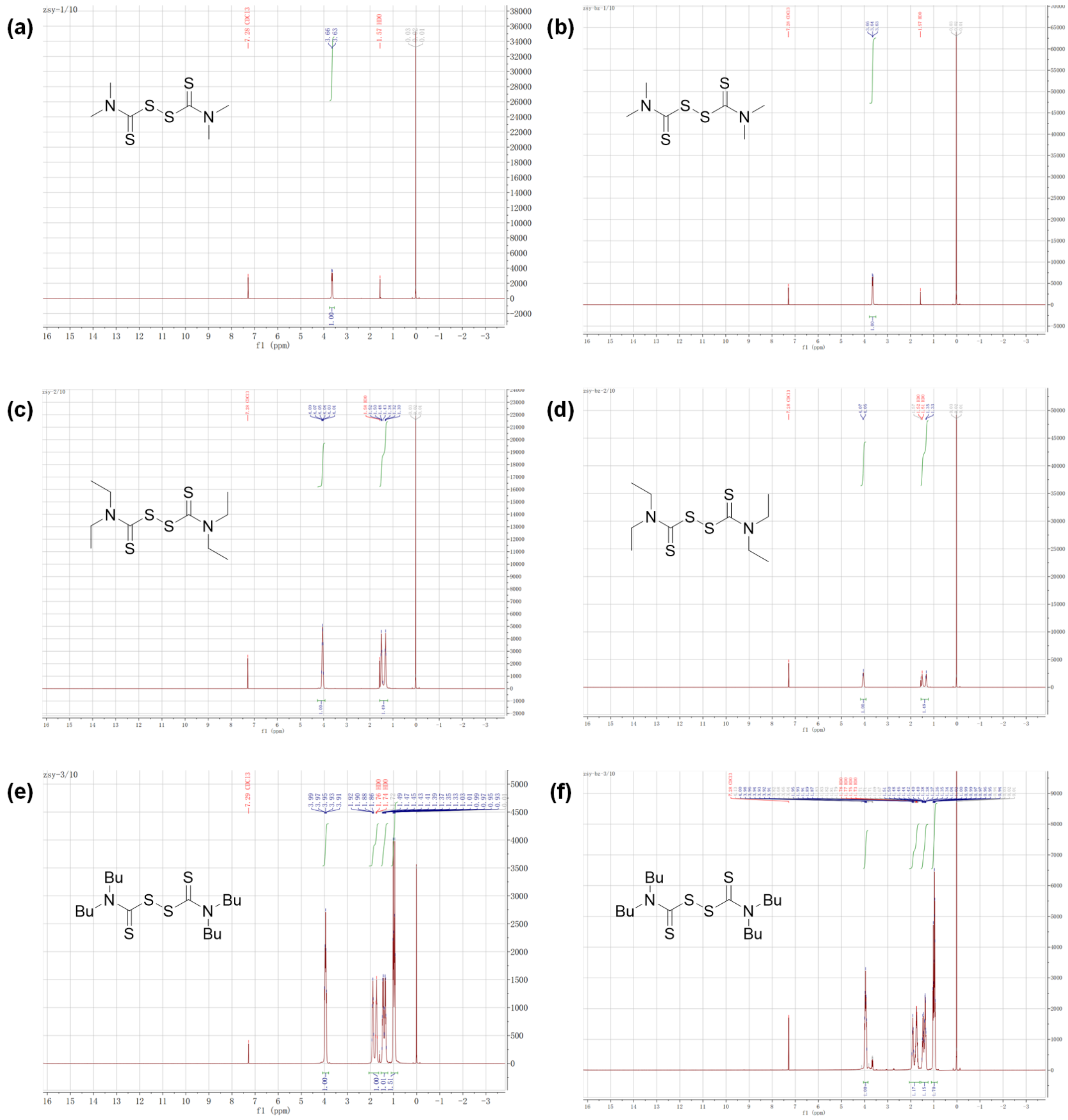

Figure S13. H^1-NMR spectra of TMTD, TETD, and TBuTD. Chloroform-d was used as the solvent. (a), (c), and (e) NMR spectra of TMTD, TETD, and TBuTD samples from microfluidic electrolysis experiments, respectively. (b), (d), and (f) NMR spectra of commercial TMTD, TETD, and TBuTD, respectively. The peak at δ = 7.3 is the impurity $CHCl_3$ in $CDCl_3$, and the peaks at δ = 1.7 is the impurity HDO in $CDCl_3$.

References

1 A. Matsuoka, K. Noishiki, K. Mae, *Chem. Eng. Sci.* **2016**, 155, 306-313.

2 M. Dang, J. Yue, G. Chen, *Chem. Eng. J*. **2015**, 262, 616-627.